RMK 31

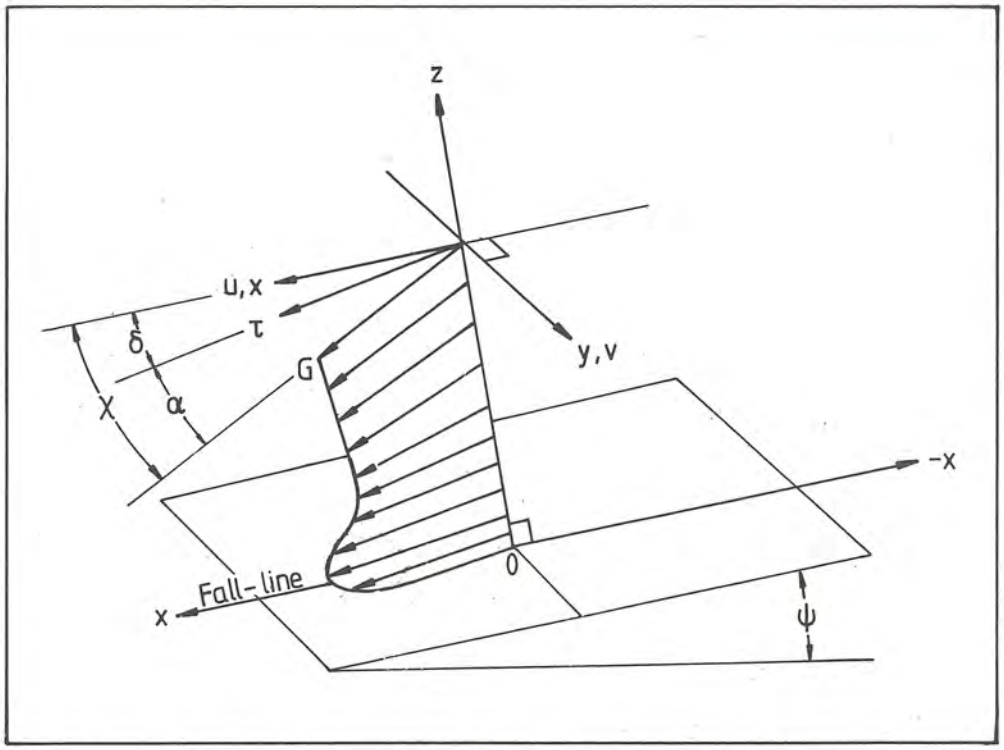


# SIMILARITY THEORY AND RESISTANCE LAWS FOR THE ATMOSPHERIC BOUNDARY LAYER

by J.W Melgarejo

SMHI SWEDISH METEOROLOGICAL AND HYDROLOGICAL INSTITUTE

**SMHI** Reports
Meteorology and Climatology

RMK 31

# SIMILARITY THEORY AND RESISTANCE LAWS FOR THE ATMOSPHERIC BOUNDARY LAYER

by J.W Melgarejo

SMHIs tryckeri, Norrköping 1983

Issuing Agency
SMHI
Box 923
S-601 19 NORRKÖPING
SWEDEN

Report number
RMK 31

Report date
September 1982

Author (s)
José W. Melgarejo

Title (and Subtitle)
Quasi-stationary structure and resistance laws of the boundary layer of time-dependent height above sloping terrain

Abstract
The theory of the boundary layer above a thermally active inclined terrain, in which the actual height h of the boundary layer is used as length scale, is presented. Analytical solutions for the mean wind and temperature structures are obtained. These solutions are seen to depend on the non-dimensional parameters h/L, $A = h_s/\lambda_s$, $h/z_o$, the slope angle $\psi$, the direction of the geostrophic wind $\chi$ in addition to z/h. As by-products of these solutions (1) expressions for the similarity theory stability functions a, b and c are obtained which are in agreement with the theoretical expressions of Zilitinkevich and Brost and Wyngaard (2). For slope angles much less than 0.01, $\psi = 0$ yields the well-known expressions of Zilitinkevich and Deardorff. The appreciable influence of $\psi$ and $\chi$ on the geostrophic drag coefficient and on the cross-isobaric angle $\alpha$ is assessed and and presented in graphical form. Finally, a preliminary test which shows that the predicted $\alpha$ is in satisfactory agreement with observations, is also presented.

Key words
Boundary layer of time-dependent height,
boundary layer above sloping terrain,
similarity theory and resistance laws of the boundary layer

Supplementary notes
Generalized formulas for the existence and heat-transfer laws are obtained which include influences of slope angle and the angle the geostrophic wind makes with the fall-line direction

Number of pages

Language
English

ISSN and title
0347-2116 SMHI Reports Meteorology and Climatology

Report available from:
Liber Grafiska AB/Förlagsorder
S-162 89 STOCKHOLM
SWEDEN

LIST OF CONTENTS


| | | Page |
|---|---|---|
| 1. | INTRODUCTION | 1 |
| 2. | FORMULATION OF THE PROBLEM | 4 |
| | a) Governing equations | 4 |
| | b) Non-dimensionalization of the equations | 6 |
| 3. | SOLUTION OF THE PROBLEM | 9 |
| 4. | DETERMINATION OF THE CONSTANTS OF INTEGRATION | 10 |
| 5. | EXPRESSIONS FOR THE RESISTANCE AND HEAT-TRANSFER LAWS | 12 |
| 6. | ASSESSMENT OF THE INFLUENCE OF $\psi$ AND $\chi$ ON THE RESISTANCE LAWS | 17 |
| 7. | COMPARISON WITH OBSERVATIONS | 26 |
| 8. | CONCLUDING REMARKS | 29 |
| | ACKNOWLEDGEMENTS | 29 |
| | LIST OF SYMBOLS | 30 |
| | REFERENCES | 31 |
| | APPENDIX | 33 |

## 1. INTRODUCTION

The problem of a stationary, horizontally homogeneous and thermally stratified turbulent atmospheric boundary layer (ABL) above a slightly inclined terrain was recently considered by Gutman and Melgarejo (1981). This ABL over a sloping terrain will be called hereafter the buoyant Ekman layer (BEL) to distinguish it from the usual Ekman boundary layer over a horizontal surface (EBL). The underlying terrain was assumed to be thermally active having an appreciable excess or deficit of heat everywhere along the slope as compared to that of the overlying air at the same level and having a constant slope angle of the order of 10 deg or less. In this case and in the case when the stratification is large, a balance between the Coriolis force, the frictional force and the 'drainage' force (component of the Archimedian force parallel to the slope) must be maintained in a non-accelerating, steady flow. From such a balance a system of one-dimensional equations that couples the EBL equations and the Prandtl 'slope wind' equations was derived. Analytical solutions were then obtained for the mean wind and temperature fields as functions of (besides $\psi$ and $\chi$) the non-dimensional height $z/\lambda_s$ and the internal parameter of stratification $\mu_s = \lambda_s/L$. [1] Here $\lambda_s$ is the length scale defined by $\lambda_s = s\, k\, u_*/f$ which is also thought of as the thickness of the stationary and horizontally homogeneous (i e equilibrium) BEL analogous to the thickness of the EBL $\lambda = k\, u_*/f$ (i e for $\psi = 0.0$) when the stratification is neutral. However, recent theoretical studies have suggested that the actual height of the ABL is a more relevant length scale.

---

[1] Notations are given in the list of symbols.

In fact, Deardorff (1972a, 1974) and Wyngaard et al (1974) have shown that for a diurnally evolving ABL its depth is not related to $\lambda$ (or $\lambda_s$). Moreover, Monin and Zilitinkevich (1974) and Zilitinkevich (1975) have shown that for an unstable ABL capped by a stably stratified atmosphere, it would take about two years to grow to its equilibrium height for an inversion strength of 4 deg/km. Therefore, it is clear why the Coriolis force must have little or no effect. On the other hand, the stable ABL would take only about a day to reach its equilibrium depth. Of course, in this latter case the effect of the Coriolis force is not negligible.

For these reasons, it is therefore expedient to generalize the model of Gutman and Melgarejo (1981) to include the actual height $h_s$ of the BEL as a length scale in lieu of $\lambda_s$ (the subscript is used to distinguish $h_s$ from h, the actual height of the EBL). As a result, the derived solutions will depend parameterically on time and horizontal coordinates (through $h_s$). The aim of this paper is thus to obtain solutions for the mean wind and temperature structures of the BEL above a sloping terrain using its actual height as an additional parameter. As by-products of these solutions, generalized expressions for the resistance and heat-transfer laws of Zilitinkevich and Deardorff (1974) will be presented. Moreover, graphical solutions showing the effects of slope and direction of geostrophic wind with respect to the fall-line vector (oriented downward along the slope, see fig 1a) on the cross-isobaric inflow angle and the geostrophic drag coefficient will be given. Lastly, comparison of model results with observations will be attempted.

a)

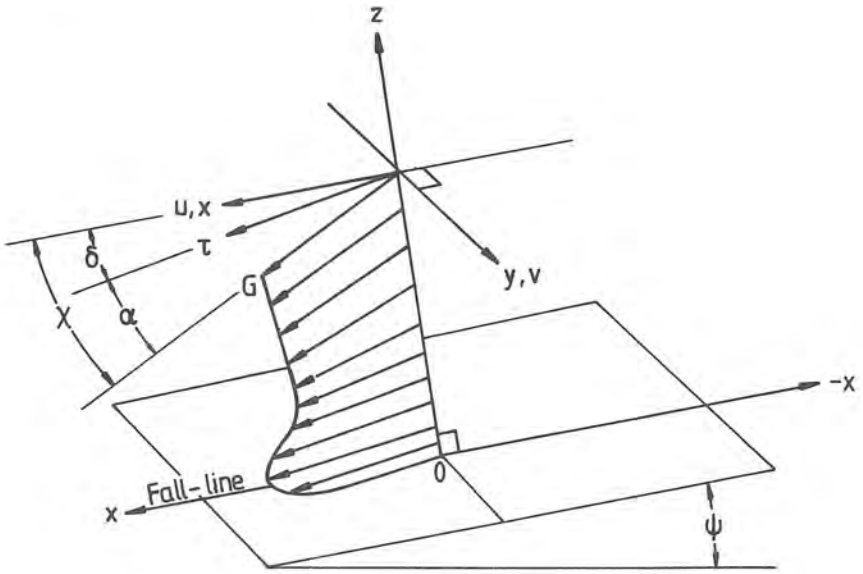


b)

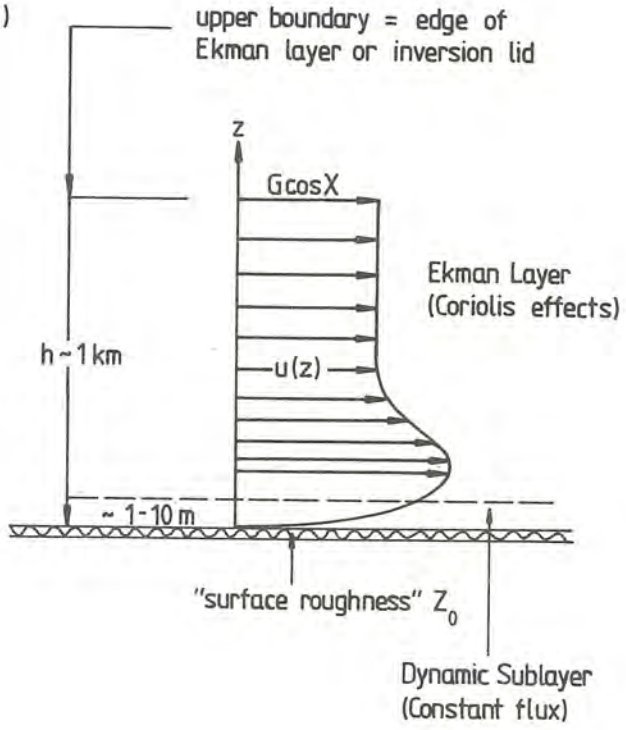


*Figures 1a and b*
*Sketch of the wind distribution in the boundary layer for the case when the sloping terrain is colder than the overlying air. a) shows the coordinate system and the sense of the angles χ, δ and α (for the Southern hemisphere). The x-axis is oriented along and the y-axis is perpendicular to the fall-line vector. The z-axis is normal to the sloping surface. b) shows the projection of the wind vector on the x-z plane.*

## 2. FORMULATION OF THE PROBLEM

### a. Governing equations

From the balance of forces in the BEL referred to above, a set of one-dimensional equations for a stationary flow is presented in Gutman and Melgarejo (1981). However, because the form of these equations may be unfamiliar and for completeness, the following form is derived in detail in the Appendix:

$$\frac{d}{dz}\left(K\frac{dp}{dz}\right) - i\frac{f}{s}p = 0 \tag{1}$$

$$\frac{d}{dz}\left(K\frac{dq}{dz}\right) = 0 \tag{2}$$

where

$$p = s(v' + \theta'\,\beta\psi/f) + iu'$$

$$q = v' - \theta'\,f/(\gamma'\psi) \quad (\gamma' = \gamma/\alpha_H) \tag{3}$$

$$s = (1 + X^2)^{-1/2};\quad X = (N'\psi/f);\quad N' = \sqrt{\beta\gamma'} \tag{4}$$

and

$$u' = u - G\cos\chi$$

$$v' = v - G\sin\chi \tag{5}$$

$$\theta' = \theta - \Theta$$

The model for eddy viscosity K is from Zilitinkevich (1970, pp 81, 204-209/

$$K = \begin{cases} \left.\begin{array}{ll} ku_*z & z \le \zeta_u L \\ \left(\dfrac{k^4\beta H}{-\zeta_u \rho c_p}\right)^{1/3} z^{4/3} & z \ge \zeta_u L \end{array}\right\} & L < 0 \\ \left.\begin{array}{ll} ku_*z & z \le L/\beta_u \\ ku_*L/\beta_u & z \ge L/\beta_u \end{array}\right\} & L > 0 \end{cases} \tag{6}$$

The physical requirement of $u = v = 0$ and $\theta' = \theta_o$ as well as the expressions for the fluxes at $z = z_o$ give from (3) and (5) the following boundary conditions:

$$\text{at } z = z_o \begin{cases} p = s(-G \sin\chi + \theta_o \beta\psi/f) - i\, G \cos\chi \\ Q = -G \sin\chi - \theta_o f/(\gamma'\psi) \\ z\frac{dp}{dz} = s\left(\frac{u_*}{k}\sin\delta - \frac{T_*}{\alpha_H}\beta\psi/f\right) + i\frac{u_*}{k}\cos\delta \\ z\frac{dq}{dz} = \frac{u_*}{k}\sin\delta - \frac{T_*}{\alpha_K} f/(\gamma'\psi) \end{cases} \qquad (7)$$

where the neutral value of the inverse turbulent Prandtl number $\alpha_H$ is introduced to facilitate comparison with the results of other investigators and the last two relationships specify the internal parameters $u_*$, $T_*$ and $\alpha$, which are also unknowns of the problem. The sense of the angles [2] $\chi$, $\delta$ and $\alpha$ and the coordinate system used is illustrated in fig. 1a.

The upper boundary conditions will be applied at the top of the BEL (instead of at infinity). Thus the assumption of $u' = v' = \theta' = 0$ at $z = h_s$ gives

$$\text{at } z = h_s \qquad p = q = 0 \qquad (8)$$

It is understandable that (8) should be approximately true for a stable BEL. In the unstable case, on the other hand, it is observed that jumps in mean potential temperature and wind fields typically develop at $h_s$ as a result of entrainment processes there. Thus following the work of Lilly (1968), Deardorff (1973) and others, it is possible to modify (8) to include these jumps. But in that case, the appearance of new parameters would make the problem more complex and it would become nearly impossible to obtain useful explicit analytical solutions (e g see Hoffert and Sud, 1976). For these reasons, then, and assuming that entrainment does not play the dominant role in shaping the mean wind and temperature profiles, (8) is retained.

---

[2] Note that $\chi$ is measured in a counter-clockwise sense from the fall-line vector. Thus $0^o$ ($360^o$), $90^o$, $180^o$ and $270^o$ are, for the geostrophic wind, in the same direction, to the left, opposite and to the right of the fall-line vector, respectively.

As to the model for K for the layers $z \leq \zeta_u L$ and $z \leq L/\beta_u$, it is consistent with the logarithmic profiles of the dynamic sublayer (see fig. 1b) which should always exist independently of stratification in the limit as $z \to 0$. As for the other two forms of K for the layers $z \geq \zeta_u L$ and $z \geq L/\beta_u$, they correspond to stratification types far from neutral, that is, when free convection sets-in in the unstable case and when an approximately constant K profile develops under very stable conditions (Belinskii, 1948 chap. 16).

## b. Non-dimensionalization of the equations

As a further development of the problem, the model equations will be non-dimensionalized using $h_s$ as the proper length scale. Here $h_s$ is assumed to be known either from observations or can be calculated by one of the theoretical or semi-empirical formulas abundant in the literature (Deardorff, 1972b, 1974; Tennekes, 1973; Benoit, 1976, Yamada, 1979; etc). Thus the following non-dimensional variables (denoted by bars), are introduced:

$$z = h_s \bar{z}; \qquad p = \frac{u_*}{k} \bar{p}; \qquad q = \frac{u_*}{k} \bar{q}$$

$$K = ku\, h_s \bar{K}; \quad z_o = h_s \bar{z}_o; \quad \bar{h}_s = 1 \tag{9}$$

Substituting (9) into (1), (2) and (6)-(8), the following non-dimensional forms of the equations (with bars ommitted hereinafter) are obtained:

$$\frac{d}{dz}\left(K \frac{dp}{dz}\right) - iAp = 0 \tag{10}$$

$$\frac{d}{dz}\left(K \frac{dq}{dz}\right) = 0 \tag{11}$$

where

$$A = fh_s/(ksu_*) = h_s = h_s/\lambda_s \tag{12}$$

From (12), it is seen that A corresponds to the parameter $hf/ku_*$ of the EBL similarity theory when h is used as length scale. To the knowledge of the author no clear physical meaning has so far been given to it although theoretical studies have appeared where the influence of this parameter on the profiles of the non-dimensional mean and internal fields has been shown for fixed values equal to or less than 1 (e g Deardorff, 1972a and Sundararajan, 1976).

That this is so can be seen from a recent work by Krishna and Arya [3] (1981), who obtained universal profiles for the non-dimensional mean velocity components and Reynolds stresses for $hf/ku_*$ near 1. On the other hand, perhaps because of the explicit appearance of f some authors have referred to A as the Coriolis effect (Hoffert and Sud, 1976) or as a measure of the relative effects of rotation and friction (Arya, 1977).

The non-dimensional form of K is

$$K = \begin{cases} z & (h_s/L \lesssim 0); \quad z \leq \nu \\ \nu^{-1/3} \, z^{4/3} & (h_s/L < 0) \\ \nu & (h_s/L > 0) \end{cases} \quad z \geq \nu \qquad (13)$$

where

$$\nu = \begin{cases} \zeta_u (h_s/L)^{-1} & (h_s/L < 0) \\ (\beta_u h_s/L)^{-1} & (h_s/L > 0) \end{cases} \qquad (14)$$

[3] Krishna, K. and S.P.S. Arya, 1981: Wind structure in neutral, entraining PBL capped by a low-level inversion: Fifth Symposium on Turbulence, Diffusion and Air Pollution, Atlanta, Ga, USA, March 9-13, 1981. American Meteorological Society. Boston, Mass 0218, USA.

The non-dimensional boundary conditions are

$$\text{at } z = z_o \quad \begin{cases} p = -sn \sin\chi + m - i\, n \cos\chi \\ q = -n \sin\chi - \dfrac{s}{1-s^2}\, m \\ z\dfrac{dp}{dz} = s \sin\delta + \alpha_H^{-1}\eta + i \cos\delta \\ z\dfrac{dq}{dz} = \sin\delta - \dfrac{s}{1-s^2}\,\alpha_H^{-1}\eta \end{cases} \tag{15}$$

and

$$\text{at } z = 1, \qquad p = q = 0, \tag{16}$$

where

$$n = \frac{kG}{u_*} \; ; \; \eta = \mu_s \frac{\psi}{k^2} \; ; \; m = \eta \frac{\theta_o}{T_*} \tag{17}$$

To complete the mathematical formulation of the problem, it is necessary to impose the following conjugate conditions at $z = \nu$ to ensure a smooth transition of solutions of the lower layer into those of the upper layer:

$$\begin{aligned} p\Big|_{z=\nu+o} &= p\Big|_{z=\nu-o} \; ; \; \frac{dp}{dz}\Big|_{z=\nu+o} = \frac{dp}{dz}\Big|_{z=\nu-o} \\ q\Big|_{z=\nu+o} &= q\Big|_{z=\nu-o} \; ; \; \frac{dq}{dz}\Big|_{z=\nu+o} = \frac{dq}{dz}\Big|_{z=\nu-o} \end{aligned} \tag{18}$$

## 3. SOLUTION OF THE PROBLEM

Since the model of K is different for the layers $z \leq \nu$ and $z \geq \nu$, analytical solutions of the system (10) and (11) for K given by (13) will be obtained separately for each layer. Then with the help of (18), these solutions will be made continuous at $z = \nu$.

The solution of (10) for $\overline{K} = \overline{z}$ is well known for its role in the theory of the resistance of conductors to alternating currents (McLachlan, 1955). The solution for $z \leq \nu$ ($\nu << 1$) and $A = 1$ is discussed in Gutman and Melgarejo (1981). Since the extension to arbitrary A is trivial, only its final form is given. Thus the solutions of (109) and (11) for $z \leq \nu$ are

$$p = (1+iAz)(C_1+C_2 \ell nz) - 2C_2 i(Az) \qquad (19)$$

$$q = c_1 + c_2 \ell nz \qquad (20)$$

$$(z_o \leq z \leq \nu;\ h_s/L \lesseqgtr 0)$$

As to the solutions of (10) and (11) for $z \geq \nu$, the unstable case will be considered first. After some elementary transformations, the solutions that satisfy (16) are

$$p = c_3 z^{-1/3} \sinh \left[3\sqrt{iA}\ \nu^{1/6}(z^{1/3}-1)\right] \qquad (21)$$

$$q = c_3(z^{-1/3} - 1) \qquad (22)$$

$$(\nu \leq z \leq 1;\ h_s/L < 0)$$

The solutions of (10) and (11) that satisfy (16) for the stable case are

$$p = C_4 \sinh \left[\sqrt{\frac{iA}{\nu}}\ (z-1)\right] \qquad (23)$$

$$q = c_4(z-1) \qquad (24)$$

$$(\nu \leq z \leq 1;\ h_s/L > 0)$$

Contrasting the solutions (19)-(24) with those of Gutman and Melgarejo (1981) it is seen that they are much the same, except that in (21) and (23) the function determining the shape of p is sinus hyperbolic (instead of exponential) as a result of applying the upper boundary conditions at $h_s$.

Solutions of the system (10) and (11) for the special case of constant K and length scale $\lambda_s$ have been obtained by Hsueh (1968, 1971) and Lykosov and Gutman (1972). They discussed at length the implications of their solutions for practical applications. It should be noted that 1) the assumption of constant K is very crude and does not allow for the correct evaluation of fluxes at $z = z_o$ and that 2) as a result of applying the upper boundary conditions at infinity they managed to solve (11) for the stable case only for the trivial case $q \equiv 0$ for all z. Therefore, it would be of value to reconsider their conclusions in the light of (19)-(24).

## 4. DETERMINATION OF THE CONSTANTS OF INTEGRATION

The constants of integration $c_1$ to $c_4$ and $C_1$ to $C_4$, real and complex respectively, appearing in (19)-(24) will now be determined. Substitution from (19) and (20) into (15) yields

$$\begin{aligned} -s\,n \sin\chi + m - i\,n\cos\chi &= C_1 + C_2 \ln z_o \\ -n\sin\chi - \frac{s}{1-s^2}\,m &= c_1 + c_2 \ln z_o \\ s\sin\delta + \alpha_H^{-1}\eta + i\cos\delta &= C_2 \\ \sin\delta - \frac{s}{1-s^2}\,\alpha_H^{-1}\eta &= c_2 \end{aligned} \qquad (25)$$

It should be noted that because of the smallness of $\bar{z}_o$, i e $\bar{z}_o = z_o/h_s \ll 1$, the first and third approximate expressions on the right side of (25) correspond to having solved (10) without the second term i e for the constant flux or dynamic sublayer (see fig. 1b) where the Coriolis force plays no role. It is seen that (25) in a sense constitutes a closed system of four equations for the four unknowns $c_1$, $c_2$, $C_1$ and $C_2$. However, since the internal parameters n, m and $\delta$ are also unknowns of the problem, (25) alone does not determine the constants of integration. Therefore, it is necessary to invoque (18) to find the additional expressions. Substituting (19)-(24) into (18), two equations for each of the unknowns $c_3$, $c_4$ and $C_3$, $C_4$ are obtained in terms of $c_1$, $c_2$ and $C_1$, $C_2$ respectively. Elimination of $c_4$ and $C_4$ from the resultant equations (for the stable case) gives, respectively

$$\begin{aligned} \frac{c_1}{c_2} &= \ln\frac{1}{\nu} - \frac{1}{\nu} + 1 \\ \frac{C_1}{C_2} &= \ln\frac{1}{\nu} - \sqrt{\frac{1}{2A\nu}} + 1 + \sqrt{\frac{A\nu}{2}} + \left(\sqrt{\frac{1}{2A\nu}} + \sqrt{\frac{A\nu}{2}}\right)i. \end{aligned} \qquad (26)$$

Similarly the elimination of $c_3$ and $C_3$ (for the unstable case) yields

$$\frac{c_1}{c_2} = \ell n \frac{1}{\nu} - 3 + 3\nu^{1/3}$$

$$\frac{C_1}{C_2} = \ell n \frac{1}{\nu} - 3 + 3\nu^{1/3} + 17A\,\nu i \qquad (27)$$

As in (25) the second expressions in (26) and (27) were obtained by eliminating terms with powers of $\nu$ greater than one.

Since (26) and (27) together with (18) determine $c_3$, $C_3$ and $c_4$, $C_4$, the solution of the problem is also completed.

Summarizing the results of sections 3 and 4, it can be said that (19)-(24) and (25)-(27) are the expressions for the quasi-stationary mean wind and temperature structures of the BEL as functions of $z/h_s$, $h_s/\lambda_s$, $h_s/L$, $h/z_o$ as well as of $\psi$ and $\chi$. By quasi-stationary is meant that the derived solutions can depend parameterically on time through $h_s$ (and $\theta_o$). No further discussion of the pecularity of the solutions nor of their dependence on the external parameters is given here since this can be the topic of another investigation.

Improvements in the model for K based on more sophisticated theories or in the formulation of upper boundary conditions to take into account the effects of entrainment, etc are not considered since they would lead only to more complicated equations with more external parameters. Even in the context of a one-dimensional model the solution of such equations is tractable usually by numerical methods. Examples of models that include these refinements for the EBL case are e g those of Kazanski and Monin (1960) and Hoffert and Sud (1976).

Thus in the opinion of the author the simple analytical solutions presented here are useful not only because they are physically transparent, but also because the effects of the external parameters can be singled out in a direct and simple way. Furthermore, from the numerical modeling point of view, analytical solutions are essential e g for purposes of testing the accuracy of numerical schemes as in the case of the classical Ekman's solutions.

## 5. EXPRESSIONS FOR THE RESISTANCE AND HEAT-TRANSFER LAWS

From the solutions obtained above, it will be shown that these can be recasted in such a way as to give expressions for $u_*/G$, $T_*/\theta_o$ and $\alpha$ in terms of $h/z_o$, $h_s/L$, $\mu_s$, N, $\psi$ and $\chi$. These expressions will be referred to as the resistance and heat-transfer laws to conform with the nomenclature in the literature. As a first step in this process, it is convenient to introduce the following definitions:

$$\frac{c_1}{c_2} = c; \quad \frac{C_1}{C_2} = b + i\,a \tag{28}$$

into (26) and (27).

Equating the real and imaginary parts and substituting $\nu$ from (14), the following expressions are obtained for the functions a, b and c:

$$\begin{aligned} a &= \sqrt{\tfrac{1}{2}\beta_u \mu_s} + 1/\sqrt{2\beta_u \mu_s} \\ b &= \ln(\beta_u h_s/L) + 1 - \sqrt{\tfrac{1}{2}\beta_u \mu_s} + 1/\sqrt{2\beta_u \mu_s} \\ c &= \ln(\beta_u h_a/L) + 1 - \beta_u h_s/L \end{aligned} \tag{29}$$

for the stable case, and

$$\begin{aligned} a &= 17\,\zeta_u/\mu_s \\ b &= \ln\left(\frac{h_s/L}{\zeta_u}\right) - 3 + 3\left[\zeta_u/(h_s/L)\right]^{1/3} \\ c &= \ln\left(\frac{h_s/L}{\zeta_u}\right) - 3 + 3\left[\zeta_u/h_s/L\right]^{1/3} \end{aligned} \tag{30}$$

for the unstable case.

That (29) and (30) are the stability functions (in this study of the internal stabilities $h_s/L$ and $\mu_s = \lambda_s/L$) will become apparent later on as will the choice of the letters a, b and c to distinguish them from the corresponding functions A, B and C of the theory that uses $\lambda_s$ alone as length scale.

Next, solving (28) for $c_1$ and $C_1$, substituting the result into (25) and equating the real and imaginary parts, the following system of three equations for the three unknowns, n, m and $\delta$ is obtained:

$$- s\, n \sin\chi + m = (b + \ell)(s \sin\delta + \eta/\alpha_H) - a \cos\delta$$

$$- n \cos\chi = (b + \ell)\cos\delta + a(s \sin\delta + \eta/\alpha_H) \qquad (31)$$

$$- n \sin\chi - \frac{s}{1-s^2}\, m = (c + \ell)(\sin\delta - \frac{s}{1-s^2}\, \eta/\alpha_H)$$

where

$$\ell = \ell n(z_o/h_s) \qquad (32)$$

and a, b and c are given either by (29) or (30). The other notations are given in previous sections.

Because of the appearance of two stability functions $\mu_s = \lambda_s/L$ (via $\eta$) and $h_s/L$, the system (31) is not closed. Perhaps for this reason Arya (1977) recommended to use the expression

$$h/L = \mu^{1/2} \qquad (33)$$

for the stable boundary layer, whereas in the unstable case (and in the middle latitudes) the relation $h_s/L \approx \mu_s$ is recommended.

In Gutman and Melgarejo (1981), it was suggested that since horizontal scales of motion and slope angles are interrelated, $\psi = f/N = 0.01$ constitutes a critical slope for boundary layer processes of mesoscale ($\psi >> 0.01$) and large scale ($\psi << 0.01$) type to occur. In that which follows, solutions of (31) for n, m and $\alpha$ for $\psi << 0.01$ only will be presented. Since this case corresponds to ABL processes of planetary scale, it becomes a very relevant study from the point of view of parameterization of the ABL for use with numerical models of large scale flow.

Thus for $\psi << 0.01$ in (4), $s \approx 1$ and therefore $h_s = h$ is obtained. Consequently, the solution of (31) for n, m and $\alpha$ for $s = 1$ (and with the notations in (17)) yields the following expressions:

$$\frac{u_*}{G} = k\left[\sqrt{(\ell n \frac{h}{z_o} - b)^2 + a^2 - (B_1\psi)^2} - B_2\psi\right]^{-1} \tag{34}$$

$$\sin\alpha = \frac{1}{kG/u_* + B_2\psi}\left[a - B_1\psi \frac{aB_1\psi + (kG/u_* + B_2\psi)(\ell n \frac{h}{z_o} - b)}{(\ell n \frac{h}{z_o} - b)^2 + a^2}\right] \tag{35}$$

$$-\frac{T_*}{\theta_o} = \alpha_H(\ell n \frac{h}{z_o} - c - B_3\psi)^{-1} \tag{36}$$

where

$$B_1 = \mu \frac{R}{D};\ B_2 = \mu \frac{R_1}{D}\ (\mu = \lambda/L;\ \lambda = k\, u_*/f)$$

$$B_3 = (R_1' \cos\alpha - R' \sin\alpha)Y\, \mu^{-1}$$

$$R = (b - c)\cos\chi - a\sin\chi;\ R' = (b - c)\cos\chi + a\sin\chi \tag{37}$$

$$R_1 = (b - c)\sin\chi + a\cos\chi;\ R_1' = (b - c)\sin\chi - a\cos\chi$$

$$D = k^2\alpha_H;\ Y = (kN/f)^2;\ N = \sqrt{\beta\gamma}$$

and a, b and c are given in (29) and (30).

Expressions (34)-(36) are the resistance and heat-transfer laws for the BEL. That they are the generalized expressions (generalized to include the effects of $\psi$ and $\chi$) of the similarity theories of Zilitinkevich and Deardorff (1974) and Melgarejo and Deardorff (1974) can be seen upon setting $\psi = 0$.

For the purpose of expressing the internal parameters solely in terms of the external parameters, it is useful to find a relationship between the external parameter of stratification, commonly denoted as the bulk Richardson number, $Ri_B$, defined by

$$Ri_B = -\beta\theta_o h/G^2 = \frac{h}{L}\left(\frac{-T_*}{\theta_o}\right)^{-1}(u_*/kG)^2 \tag{38}$$

and the internal stratification parameter h/L.

Substituting of (34) and (36) into (38) gives

$$Ri_B = \frac{h}{L}\alpha_H^{-1}\frac{(\ell n\frac{h}{z_o} - c - B_3\psi)}{\left[\sqrt{(\ell n\frac{h}{z_o} - b)^2 + a^2 - (B_1\psi)^2} - B_2\psi\right]^2} \qquad (39)$$

Thus setting $\psi = 0$ in (34)-(36) and (39), the well-known equations of Zilitinkevich and Deardorff (1974) are recovered [4]:

$$\left.\begin{aligned} \frac{u_*}{G} &= k\left[(\ell n\frac{h}{z_o} - b)^2 + a^2\right]^{-1/2} \\ \sin\alpha &= \frac{a}{k}(u_*/G) \\ -\frac{T_*}{\theta_o} &= \alpha_H(\ell n\frac{h}{z_o} - c)^{-1} \\ Ri_B &= \frac{h}{L}\alpha_H^{-1}\frac{(\ell n\frac{h}{z_o} - c)}{(\ell n\frac{h}{z_o} - b)^2 + a^2} \end{aligned}\right\} \quad (\psi = 0) \qquad (40)$$

Comparing (34)-(36) with (40), it can be seen that the a, b and c stability functions contained therein are exactly the same (independent of $\psi$). This means that although the slope affects the argument of these function as seen from (29) and (30), their shape remains the same.

It is also of interest to solve (31) for the function a, b and c instead for m, n and $\alpha$. Thus for s = 1, the solutions are

$$a = \frac{(kG/u_*)\sin\alpha - \psi\eta'(\frac{\alpha_H\theta_o}{T_*}\cos\delta + \frac{kG}{u_*}\cos\chi)}{1 + \psi\eta'(2\sin\delta + \psi\eta')} \qquad (41)$$

$$b = n\frac{h}{z_o} - \frac{(kG/u_*)\cos\alpha + \psi\eta'\left[\frac{\alpha_H\theta_o}{T_*}(\sin\delta + \eta'\psi) - n\sin\chi\right]}{1 + \psi\eta'(2\sin\delta + \psi\eta')} \qquad (42)$$

$$c = \ell n\frac{h}{z_o} + \frac{\alpha_H\theta_o/T_* + \psi S(kG/u_*)\sin\chi}{1 - \psi S(kG/u_*)\sin\delta} \qquad (43)$$

[4] Note that the sign of $\theta_o$ in this paper is + if unstable and - if stable.

where

$$\eta' = \mu/D$$
$$S = \mu^{-1}Y \qquad (44)$$

and D and Y are given in (37). The relationship between $\delta$ and $\alpha$ is $\delta = \chi - \alpha$ as seen from fig. 1a.

Upon setting $\psi = 0$ in (41)-(43), as in (40) the following expressions are obtained:

$$\left.\begin{aligned} a &= (kG/u_*)\sin\alpha \\ b &= \ell n\,\frac{h}{z_o} - (kG/u_*)\cos\alpha \\ c &= \ell n\,\frac{h}{z_o} + \alpha_H\,\theta_o/T_* \end{aligned}\right\} \quad (\psi = 0) \qquad (45)$$

It can be seen that (45) are the same expressions as those used by e g Melgarejo and Deardorff (1974, 1975), Arya (1974), Clarke and Hess (1974), Yamada (1976) and Garrat and Francey (1978). Thus (41)-(43) are the generalized expressions for the a, b and c functions which include the effects of $\psi$ and $\chi$. It would be interesting to evaluate these functions from experimental data in the light of (41)-(43) since the terms associated with $\psi$ and $\chi$ are comparable in magnitude to the remaining terms even for $\psi$ as small as 0.001.

In closing this section it should be noted that the expressions for the a, b and c functions derived in the present paper for the models of turbulence in (13) and presented in (29) and (30) are in agreement with the theoretical results of Zilitinkevich (1975) and those of Wyngaard (1975) and Brost and Wyngaard (1978) for the stable case, except for the differences in the multiplying constant coefficients.

## 6. ASSESSMENT OF THE INFLUENCE OF $\psi$ AND $\chi$ ON THE RESISTANCE LAWS

As an example in this study, a graphical representation of the solutions (34)-(36) will be given only for the special case of $h/L = \mu$. To this end, the best-fit polynomials for a, b and c of Yamada (1976) derived from the 'Wangara' data of Clarke et al (1971) will be used. These functions are expected to be closer to reality than those in (29) and (30) because the latter contain many of the simplifying assumptions introduced in the formulation of the present problem.

From these considerations it is seen that one important advantage of the method of obtaining solutions as presented here is this possibility of incorporating into the solutions observed information through the a, b and c functions.

For completeness the empirical functions of Yamada (1976) used in the calculations are included here. They are, for the stable case

$$\left.\begin{aligned}
a &= 3.02 + 0.3\, h/L && ;\ 0 \le h/L \le 35 \\
&= 2.85\,(h/L - 12.47)^{1/2} && ;\ h/L > 35 \\
b &= 1.855 - 0.38\, h/L && ;\ 0 \le h/L \le 35 \\
&= -2.94\,(h/L - 19.94)^{1/2} && ;\ h/L > 35 \\
c &= 3.665 - 0.829\, h/L && ;\ 0 \le h/L \le 18 \\
&= -4.32\,(h/L - 11.21)^{12} && ;\ h/L > 18
\end{aligned}\right\} \quad h/L \ge 0 \text{ (stable)} \qquad (46)$$

and for the unstable case

$$\left.\begin{aligned}
a &= 3.020\,(1 - 3.29\, h/L)^{-1/3} \\
b &= 10.0 - 8.145\,(1.0 - 0.008376\, h/L)^{-1/3} \\
c &= 12.0 - 8.335\,(1.0 - 0.03106\, h/L)^{-1/3}
\end{aligned}\right\} \quad h/L \le 0 \text{ (unstable)} \qquad (47)$$

The graphical representation is also given in fig. 2. An indication of their close agreement with reality is suggested by Yamada's (1976) Figs. 15 and 16, which show good agreement between the computed and observed non-dimensional velocity defect profiles.

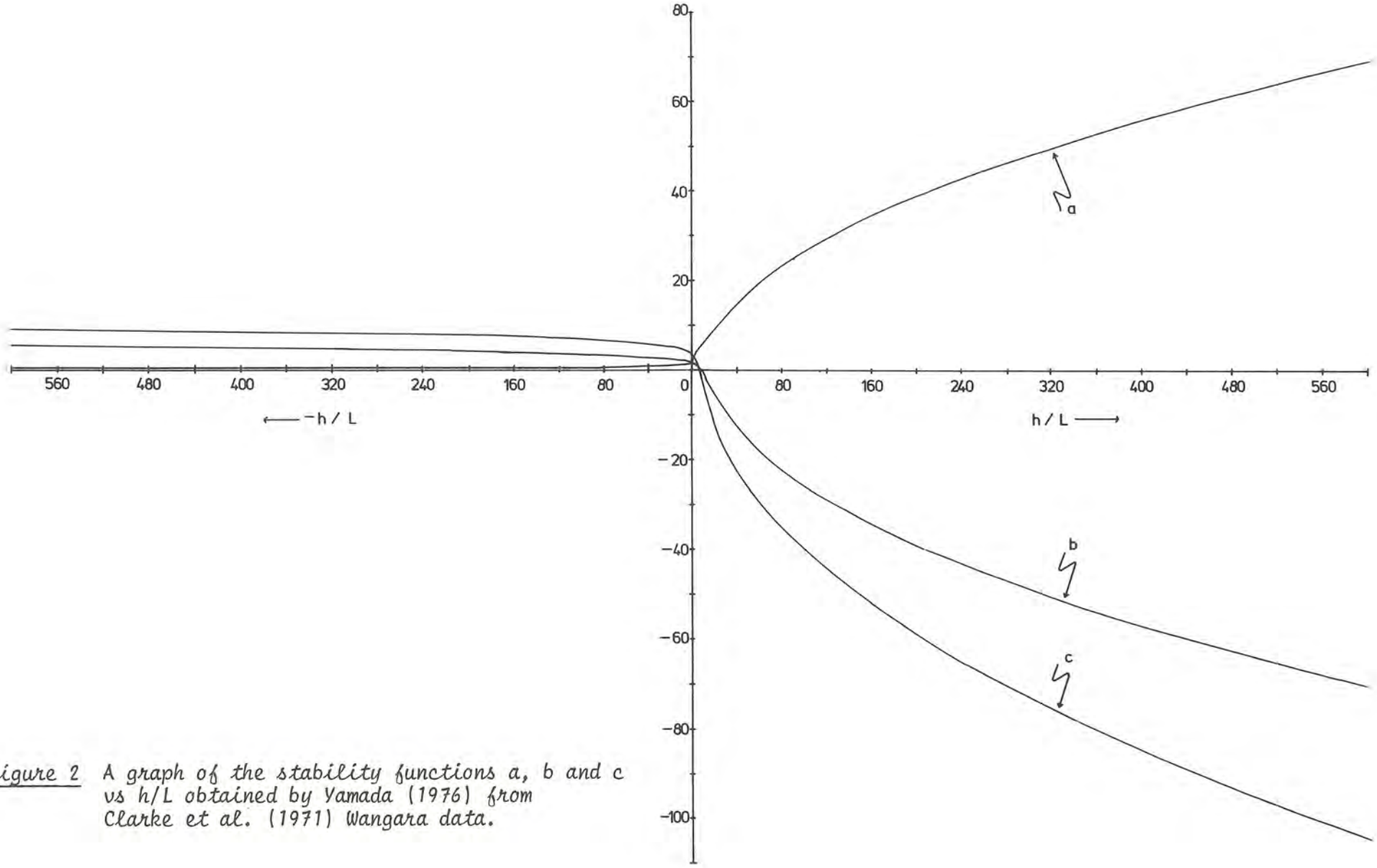


*Figure 2* A graph of the stability functions a, b and c vs h/L obtained by Yamada (1976) from Clarke et al. (1971) Wangara data.

The dependence of $u_*/G$ on $h/z_o$ for different values of $\psi$ and for fixed h/L and $\chi$ is presented in Fig. 3 for the range of $h/z_o$ of meteorological interest. The interesting result to be noted is that the effect of $\psi$ increases as $h/z_o$ decreases (or as $z_o$ increases) and that the departure from the curve for $\chi = 0$ increases as $\chi$ increases. The curves for other combinations of h/L and $\chi$ showed the same behaviour and are therefore not presented. It should be pointed out here that (34) guarantees positive solutions only for $\psi$ values less than a certain upper limit, which depends on all the other parameters but mostly on h/L. In the present study it was found that (34) will give non-negative values always for $\psi \lesssim 0.003$ and $|h/L| \lesssim 230$. This is the reason for choosing $\psi = 0.001$ as an upper limit. The fact that (34) does not always guarantee positive solutions is to be expected in the context of the present simple model where e g non-linear effects are not considered. The peculiarity of (34) is also found in the corresponding equation for $u_*/G$ in the Rossby number similarity theory for the EBL (Zilitinkevich and Monin, 1974).

Fig. 4 shows $u_*/G$ as a function of $\chi$ and h/L for fixed values of $\chi$ and $h/z_o$. The effect of $\chi$ is to produce an oscillatory curve of non-equal positive and negative amplitudes around the value of $u_*/G$ for $\psi = 0$. It is also seen that larger amplitudes correspond to larger h/L values as expected. The effect of increasing $h/z_o$ or decreasing $\psi$ was to decrease the amplitudes as seen from Fig. 3. Also shown is that the position of the maxima and minima is independent of h/L and $h/z_o$. That is, their position for a fixed $\psi$ depends only on the orientation of G with respect to the fall-line vector.

Since the positions of these maximum and minimum points can be reflection of the particular formulas for a, b and c used, no precise evaluation from (34) of the values of $\chi$ corresponding to these positions is given. These and other peculiarities of the curves can partly be explained by simple physical considerations, e g the conflicting or complementary (depending on $\chi$ as well as on the sign and magnitude of h/L) action of the pressure gradient and drainage forces.

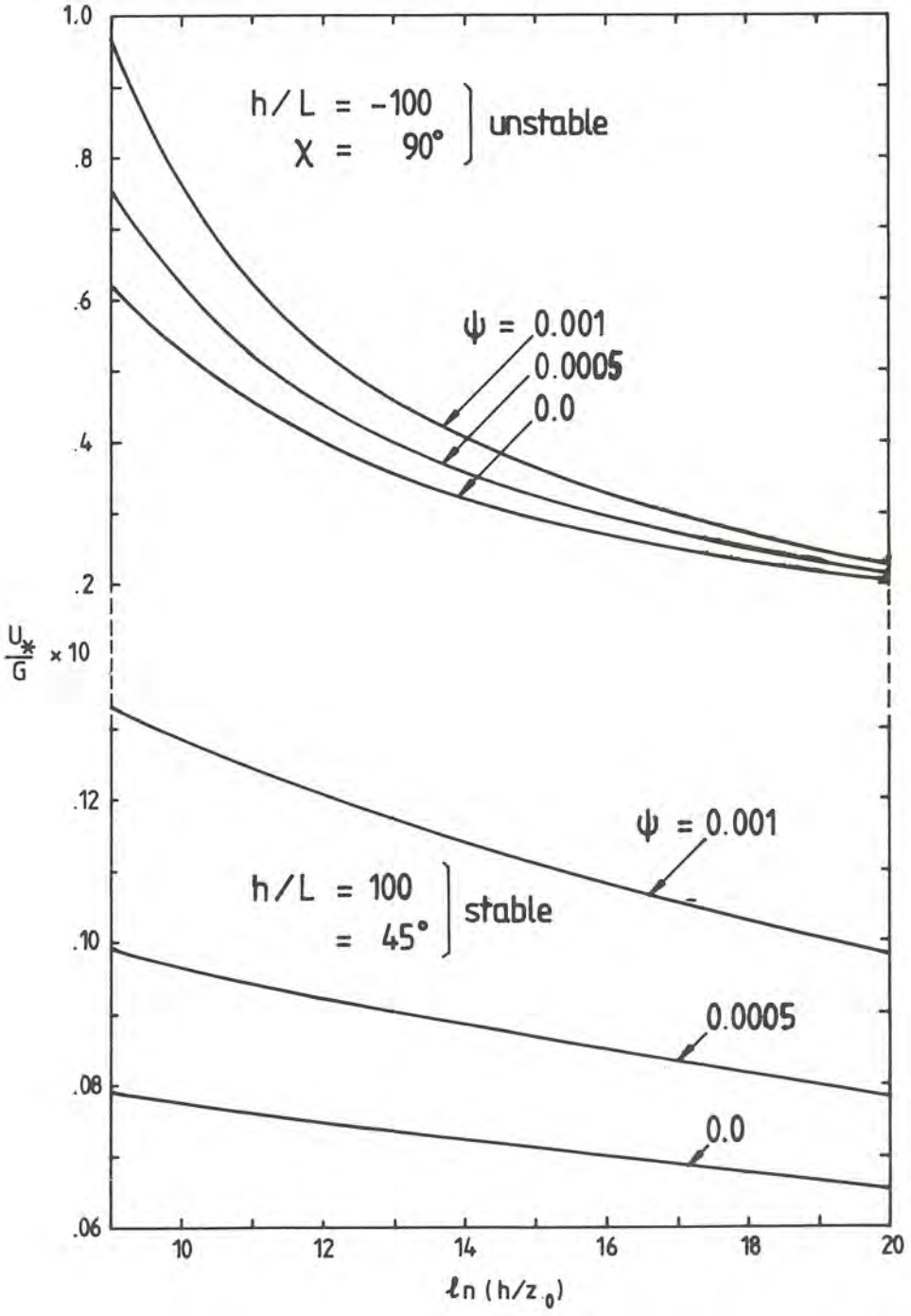


*Figure 3* *Nomogram of the geostrophic drag coefficient, $u_*/G$ vs $\ln(h/z_0)$, for three values of the slope angle $\psi$ i e 0, 0.0005 and 0.001 and for fixed h/L and $\chi$.*

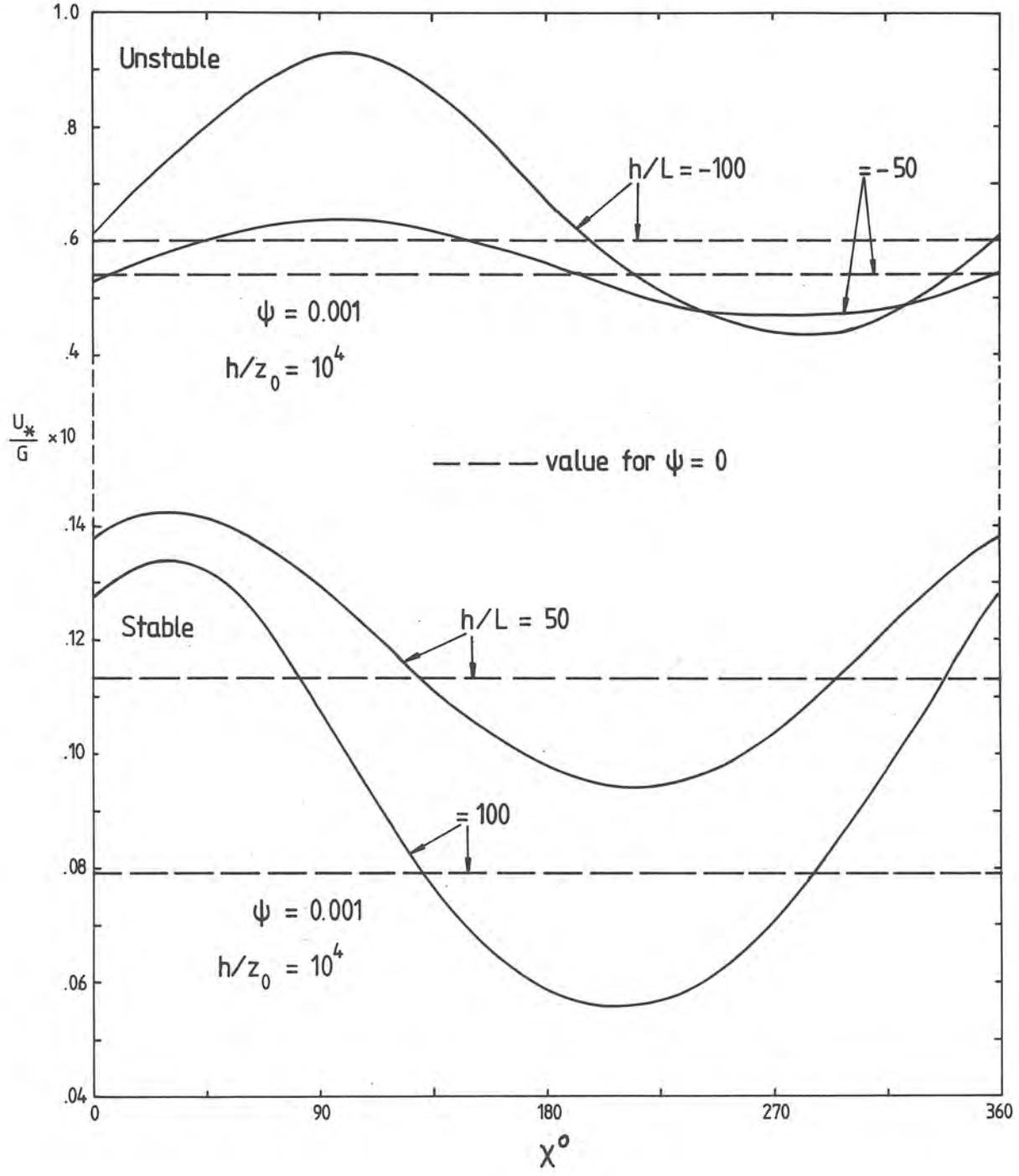


*Figure 4* *Nomogram of $u_*/G$ vs $\chi$ for $|h/L| = 50$, 100 and for $\psi$ and $h/z_0$, fixed to 0.001 and $10^4$ respectively.*

Fig. 5 is similar to Fig. 3 except for $\alpha$ (for sign f = -1). The effect of $\psi$ on $\alpha$ (for fixed h/L and $\chi$) is the same as that on $u_*/G$ in the stable case. However, when the stratification is unstable and for a certain orientation of the geostrophic wind $\alpha$ is observed to become negative, implying BEL flow towards high pressure. This is a novel result of the present theory which is not predicted by the simpler EBL theory. This interesting result is examined more closely in Fig. 6, which is a diagram of $\alpha$ as a function of $\chi$ and h/L for fixed $\psi$ and $h/z_o$. It is seen that a negative $\alpha$ occurs for two ranges of $\chi$. The positions of the maximum positive and negative amplitudes, with respect to $\alpha = 0$, are observed to be independent of h/L and $h/z_o$ (shown in Fig. 7) for a fixed value of $\psi$. Nomograms for $\psi <$ 0.001 showed the same behaviour except for smaller amplitudes. The dependence of 0-line crossing points on $\chi$ and h/L is shown in Fig. 7 for $\psi =$ 0.001. The interesting features of the figure are that no negative $\alpha$ (or flow towards high pressure) occurs for geostrophic wind orientation between approximately $90^\circ < \chi < 270^\circ$ and that the tendency for $\alpha$ to become negative (in the allowable range of $\chi$) decreases as - h/L decreases. This behaviour of $\alpha$ suggests the existence of a lower limit for - h/L where $\alpha$ becomes negative for all values of $h/z_o$. Since the 0-line crossing points are independent of $h/z_o$, the calculations of $\chi$ for $\alpha = 0$ is in order. Thus setting $\alpha = 0$ in (35), the following quadratic equation for $\chi$ is obtained:

$$\cos\chi = a\left[\frac{E(b-c) \pm \sqrt{(b-c)^2 + a^2\,(1-E^2)}}{(b-c)^2 + a^2}\right] \qquad (48)$$

where

$$E = D\left(\frac{h}{L}\,\psi\right)^{-1}$$

The solution of (48) for $\psi = 0.001$, for the a, b and c functions given by (47) and for - h/L = 50, 100 and 200 gives the following values for $\chi$ rounded to the nearest integer: $65^\circ$ and $314^\circ$, $85^\circ$ and $289^\circ$, $91^\circ$ and $280^\circ$, respectively (as shown in Fig. 7). Note that a = 0 in (48) gives $\chi = 90^\circ$ and $270^\circ$ for the 0-line crossing points. That these theoretical values are in close agreement with those shown in Fig. 7 for - h/L = 200 is to be expected since $\pm$ values used in the calculations were $a \approx 0$ for - $h/L \geq 80$ (see Fig. 2). As is the case with (34) for $u_*/G$, solutions of (35) have physical meaning ($|\alpha| \leq 90^\circ$) only for $|h/L| \lesssim 230$ and $\psi \lesssim 0.003$.

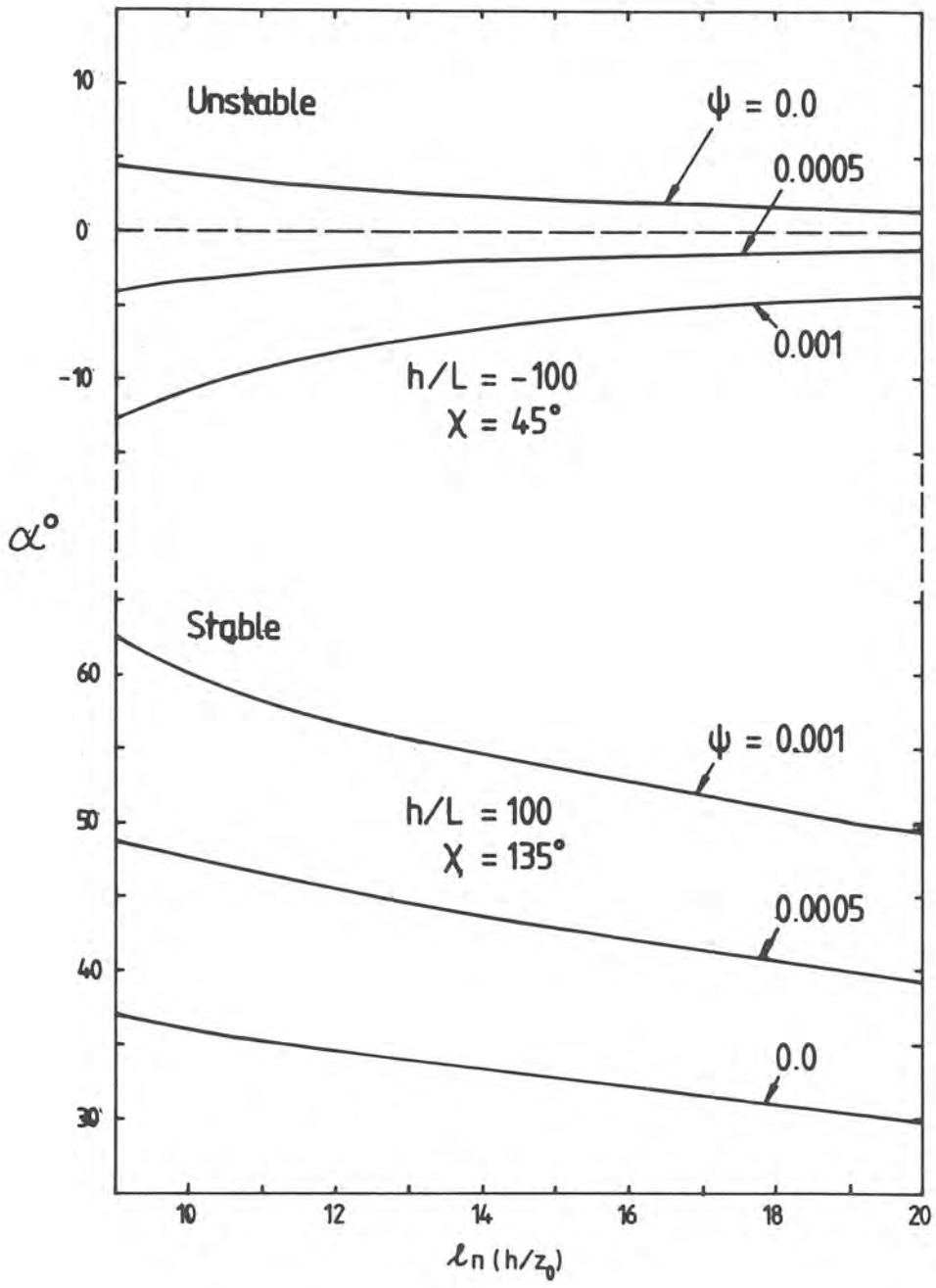


*Figure 5* The same as Fig. 3 except for the cross-isobaric angle $\alpha$ and different choices of $\chi$.

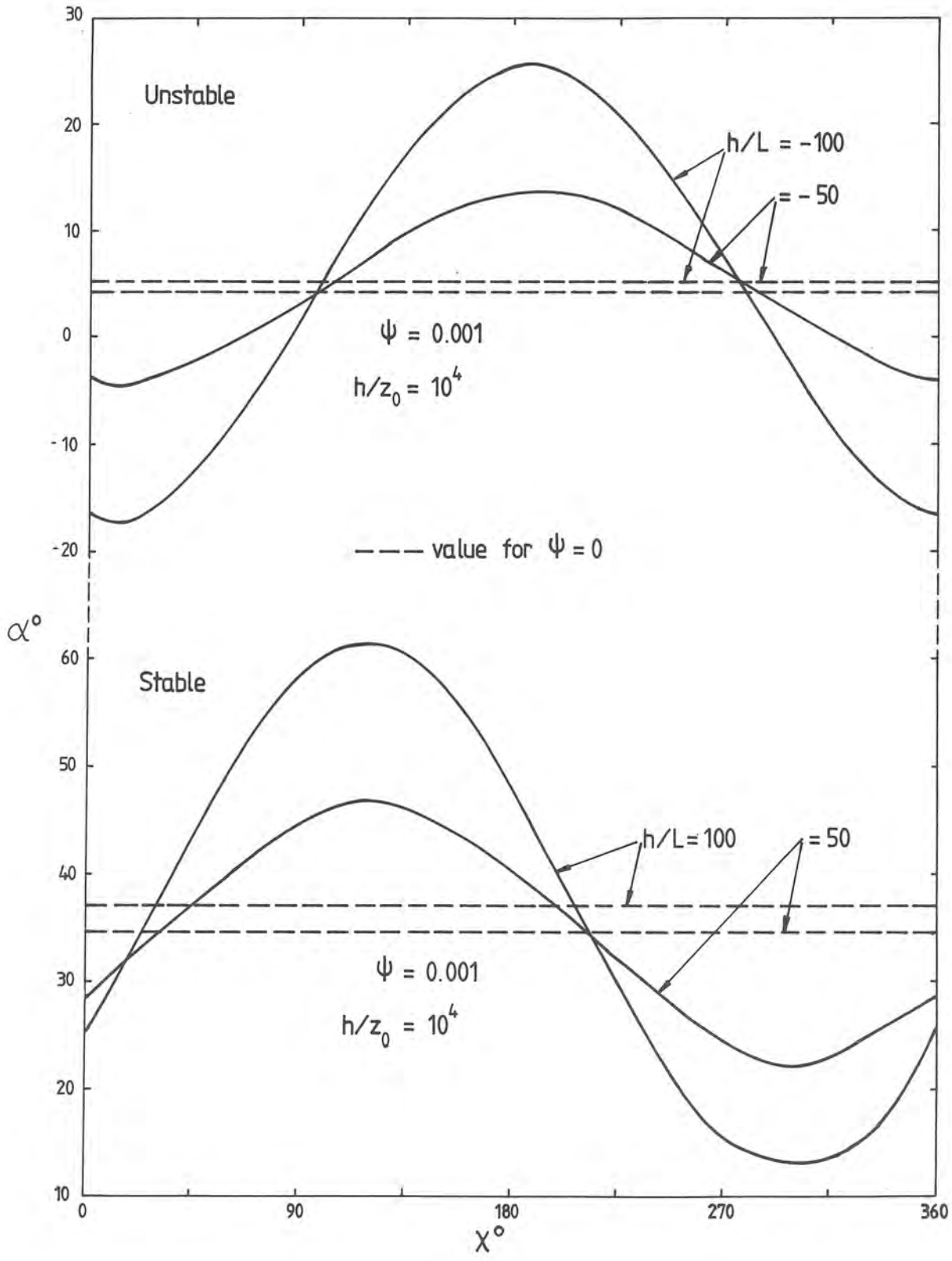


*Figure 6* The same as Fig. 4 except for α.

Before leaving this section it should be pointed out that 1) the choice of the particular values of $h/L$, $h/z_o$, $\psi$ or $\chi$ in Fig. 3 is made for the purpose of bringing out their maximum influences which occur at these values, 2) no complete explanation of the results is offered since it would be outside the scope of the present paper. Due to lack of theoretical results of the influences of $\psi$ and $\chi$ on the resistance and heat-transfer laws of the type presented here, no comparison of the results of this investigation with those of others is offered.

The influences of $\psi$ and $\chi$ on the resistance and heat-transfer laws for the special case of $G = 0$, absence of Coriolis force and $\psi \gg 0.01$ is given in Gutman and Melgarejo (1981). It is to be noted that for this special case, $\gamma$ becomes an important parameter.

## 7. COMPARISON WITH OBSERVATIONS

Melgarejo and Deardorff (1974), when evaluating the stability functions a, b and c from the Wangara data, found that in many of the unstable cases examined, the cross-isobaric flow was towards high pressure. This implies negative $\alpha$ angles and therefore also negative $\underline{a}$ as can be seen from their Fig. 2 computed with the second equation in (40). This observed fact of negative $\alpha$ is interpreted here as due to the effect of the slope of the Wangara site. The presence of a definite slope of this site can be clearly seen from topographical maps of the area. On the other hand, the present theory predicts $\alpha$ to be negative over a slightly inclined terrain that is warmer than the overlying air and in the presence of geostrophic wind blowing either to the left or right of the fall-line vector. Therefore it is of interest to compare the model results with some of the observations mentioned above.

For this purpose, preliminary calculations for $\psi$ and the fall-line vector direction were made giving respectively 0.001 and ~ $65^{\circ}$ from E, pointing positive in a SW direction. Although explanations of the observed nocturnal accelerations at Wangara have been given assuming a slope of $7 \times 10^{-3}$ ascending towards east by L. Mahrt (personal communication), no other work has appeared (to the knowledge of the author) where the slope and fall-line vector of the Wangara site have been determined to contrast the values given above. The data points chosen for the comparison are those analyzed by Melgarejo and Deardorff (1974, 1975) and are entered in Table 1. Only those points for which - h/L falls within the validity of the predictions of the present theory have been included. These are plotted in Fig. 7 taking the observed values of $\chi$ along the abscissa and the corresponding observed values of $\alpha$ along the coordinate. The parameters h and L which are also included in Table 1 are taken from Melgarejo and Deardorff (1974) and (1975) respectively. Note that the values of $\alpha$ and $\chi$ (in Table 1) were obtained using the surface geostrophic winds reported by the synoptic network stations for every 3 hours.

Fig. 7 shows clearly that there is correspondence between the predicted and observed angles $\alpha$ (at Wangara). This result is taken here as satisfactory and encouraging for further work considering the uncertainties involved, e g in the determination of h, L, $z_o$, $\psi$ and the measurement of the geostrophic wind. The parameters h/L and $h/z_o$ that can be read off from the diagram (for the data points) are also found in satisfactory agreement with the corresponding h/L and $h/z_o$ which can be computed from Table I.

*Table 1*

*Wangara Parameters*

| Day | Hour | h (m) | -L (m) | α (deg) | χ (deg) |
|---|---|---|---|---|---|
| 1 | 15 | 1150 | 37.9 | -5 | 63 |
| 6 | 15 | 600 | 0.7 | 11 | 325 |
| 7 | 12 | 350 | 17.7 | -3 | 41 |
| | 15 | 850 | 12.3 | -18 | 42 |
| 12 | 12 | 925 | 20.8 | 0 | 264 |
| 13 | 12 | 800 | 32.1 | -19 | 300 |
| | 15 | 950 | 27.2 | 9 | 321 |
| 14 | 15 | 750 | 6.3 | -47 | 316 |
| 25 | 15 | 1150 | 28.6 | 6 | 149 |
| 26 | 12 | 475 | 45.5 | 24 | 64 |
| | 15 | 900 | 36.7 | 17 | 55 |
| 33 | 12 | 1000 | 1.5 | 1 | 283 |
| | 15 | 1150 | 2.8 | 23 | 286 |
| 34 | 12 | 600 | 15.7 | -18 | 319 |
| | 15 | 750 | 14.8 | 17 | 323 |
| 35 | 12 | 875 | 40.2 | -3 | 332 |

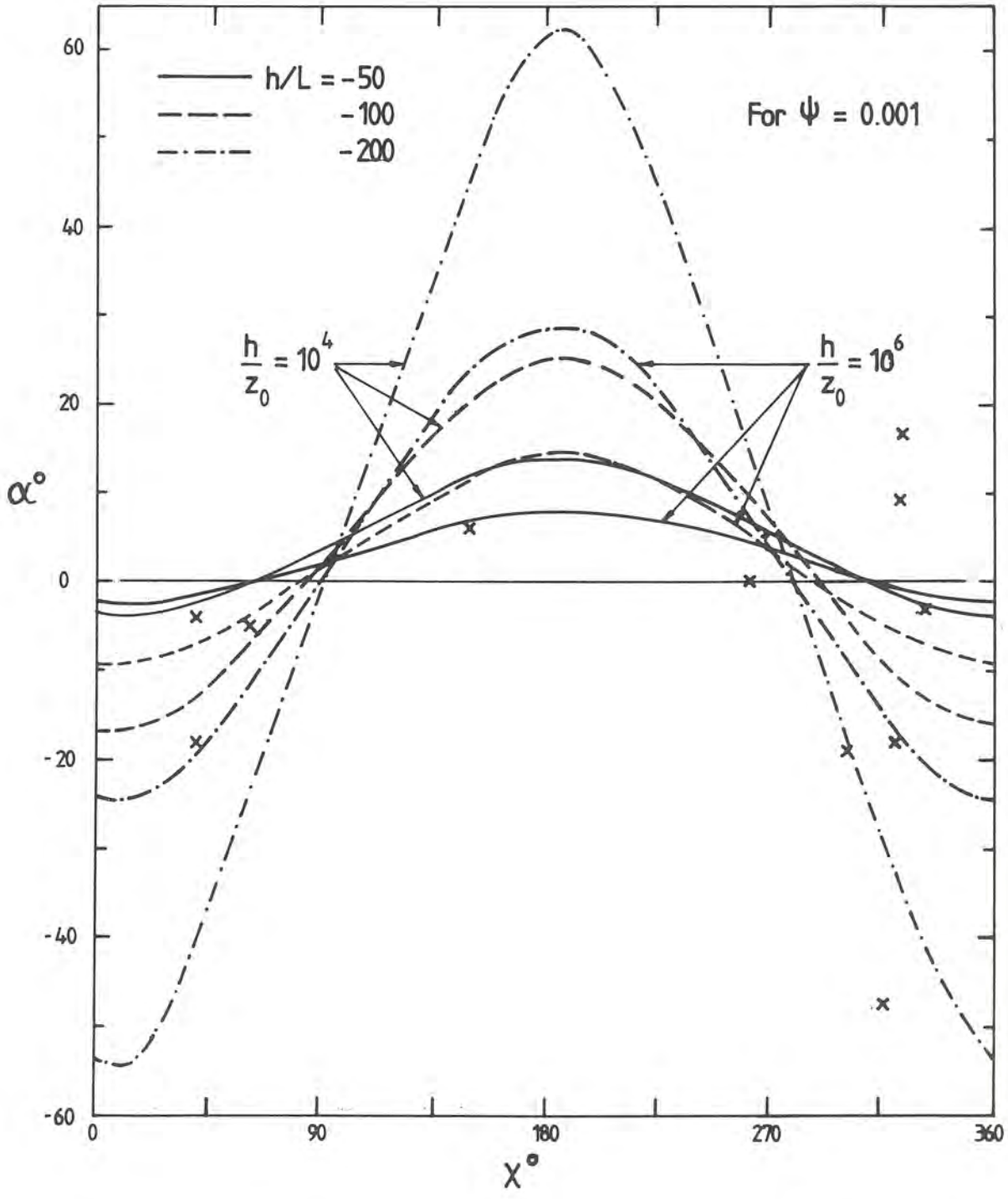


*Figure 7* Nomogram of $\alpha$ vs $\chi$ for the unstable case, for three values of $-h/L$ i e 50, 100, 200 and for two values of $h/z_0$ i e $10^4$ and $10^6$

## 8. CONCLUDING REMARKS

The problem of an ABL above a thermally active inclined plane was considered. The physical height $h_s$ of the boundary layer was introduced as the length scale in the formulation of the present problem. The use of $h_s$ is to be viewed as a further development of the theory developed by Gutman and Melgarejo (1981). For a simplified model of turbulence, analytical solutions for the mean wind and temperature structures were obtained. These solutions were seen to depend on the non-dimensional parameters $h_s/\lambda s$, $h_s/z_o$, $h_s/L$, $\psi$ and $\chi$ as well as on the variable $z/h_s$ and are to be viewed as a generalization of the Prandtl slope wind solution and the usual EBL solutions.

As by-products of these solutions, analytical expressions for the stability functions a, b and c were obtained in agreement with the theoretical findings of other investigators. Furthermore, with the aid of the logarithmic solutions of the dynamic sublayer, expressions for the resistance and heat-transfer laws above a sloping surface were derived. That these expressions are a generalization of those derived by Zilitinkevich and Deardorff (1974) was also shown.

For the stability functions derived from observations by Yamada (1976), the appreciable dependence of $u_*/G$ and $\alpha$ not only on $\psi$ but also on $\chi$ was presented in Figs. 3-7. A preliminary test of the predicted $\alpha$ against observations (that call for further tests of the predictions of this theory with observations) was given in Fig. 7. Further comparisons of $\alpha$, $u_*/G$ and $T_*/\theta_o$ are left as topics for further research. Finally, the more accurate determination of $\psi$ and $\chi$ for the Wangara site will give the possibility of reevaluating the stability functions a, b and c found by Melgarejo and Deardorff (1974, 1975), Yamada (1976), etc, in the light of (41)-(44).

## ACKNOWLEDGEMENTS

The author would like to express his sincere gratitude to Professor L N Gutman for making possible a visit to the University of Tel-Aviv, Israel, where the idea for this paper was conceived, to Professor Bert Bolin and Docent Hilding Sundqvist for their comments which helped to shape the final version of this paper, to Barbro Liensdorf and Kerstin Fabiansen for skilfully typing the manuscript and to Anita Bergstrand and Gun-Britt Rosén for drawing the final figures.

# L I S T  O F  S Y M B O L S

| | |
|---|---|
| $c_p$ | specific heat of air at constant pressure |
| $f$ | the Coriolis parameter |
| $G$ | modulus of the geostrophic wind |
| $H$ | surface value of heat flux |
| $i$ | $\sqrt{-1}$ |
| $k$ | Karman constant set to 0.35 in the calculations (Businger et al., 1971) |
| $L$ | Monin-Obukhov length = $u_*^2/(k^2\beta T_*)$ |
| $R$ | gas constant for dry air |
| $T_*$ | friction temperature = $- H/(k\rho c_p u_*)$ |
| $u_*$ | friction velocity |
| $z_o$ | roughness parameter |
| $\alpha$ | cross-isobaric inflow angle |
| $\alpha_H$ | neutral value of inverse turbulent Prandtl number set to 1.35 in the calculations (Businger et al., 1971) |
| $\beta$ | buoyancy parameter = $g/\Theta_o$ |
| $\beta_u$ | an empirical constant = 10 (Zilitinkevich and Chalikov, 1968) |
| $\gamma$ | vertical gradient of potential temperature in the free atmosphere |
| $\delta$ | angle between the surface wind vector and the x-axis |
| $\Theta$ | potential temperature of the free atmosphere |
| $\Theta_s$ | its value at the surface |
| $\theta$ | total potential temperature |
| $\theta_o$ | its average value in the ABL, a constant |
| $\zeta_u$ | an average constant = -0.07 (Zilitinkevich and Chalikov, 1968) |
| $\psi$ | terrain slope angle |
| $\chi$ | angle between the geostrophic wind vector and the fall-line vector |

REFERENCES


Arya, S.P.S., 1974: Geostrophic drag and heat transfer relations for the atmospheric boundary layer. Quart. J. Roy. Meteor. Soc., 101, 147-161.

Arya, S.P.S., 1977: Suggested revisions to certain boundary layer parameterization schemes used in atmospheric circulation models. Mon. Wea. Rev., 105, 215-227.

Benoit, R., 1976: A comprehensive parameterization of the atmospheric boundary layer for general circulation models. NCAR Cooperative Thesis No. 39. National Center for Atmospheric Research and McGill University.

Belinskii, V.A., 1948: Dynamic Meteorology, OGIZ, State Publishing House of Technical-Theoretical Literature, Moscow-Leningrad. English translation by the Israel Program for Scientific Translations, 1961.

Brost, R.A. and J.C. Wyngaard, 1978: A model study of the stably stratified planetary boundary layer. J. Atmos. Sci., 35, 1427-1440.

Businger, J.A., J.C. Wyngaard, Y. Izumi and E.F. Bradley, 1971: Flux-profile relationships in the atmospheric surface layer. J. Atmos. Sci., 28, 181-189.

Clarke, R.H., A.J. Dyer, R.R. Brook, D.G. Reid and A.J. Troup, 1971: The Wangara Experiment: Boundary layer data. Tech. Paper No. 19, Div. Meteor. Phys. CSIRO, Aspendale Vic. 3195, Australia.

Clarke, R.H. and G.D. Hess, 1974: Geostrophic departure and the functions A and B of Rossby-number similarity theory. Bound.-Layer Meteor., 7, 267-287.

Deardorff, J.W., 1972a: Numerical investigation of neutral and unstable planetary boundary layer. J. Atmos. Sci., 29, 91-115.

Deardorff, J:W., 1972b: Parameterization of the planetary boundary layer for use in general circulation models. Mon. Wea. Rev., 100, 93-106.

Deardorff, J.W., 1973: An explanation of anomalously large Reynolds stresses within the convective planetary boundary layer. J. Atmos. Sci., 30, 1070-1076.

Deardorff, J.W., 1974: Three-dimensional numerical study of the height and mean structure of a heated planetary boundary layer. Bound.-Layer Meteor., 7, 81-106.

Garrat, J.R. and R.J. Francey, 1978: Bulk characteristics of heat transfer in the unstable barocline atmospheric boundary layer. Bound.-Layer Meteor., 15, 399-421.

Gutman, L.N. and J.W. Melgarejo, 1981: On the laws of geostrophic drag and heat transfer over a slightly inclined terrain. J. Atmos. Sci., 38,1713-1724.

Hoffert, M.I. and Y. sud, 1976: Similarity theory of the buoyantly interactive planetary boundary layer with entrainment. J. Atmos. Sci., 33, 2136-2151.

Hsueh, Y., 1969: Buoyant Ekman layer. The Physics of Fluids, 12, 1757-1762.

Hsueh, Y., 1970: A note on the boundary layer wind structure above sloping terrain. J. Atmos. Sci., 27, 322-327.

Kazanski, A.B. and A.S. Monin, 1960: A turbulent regime above the ground atmospheric layer. Bull. (Izv.) Acad. Sci. USSR, Geophys. Ser., No. 1.

Lilly, D.K., 1968: Models of cloud-topped mixed layers under a strong inversion. Quart. J. Roy. Meteor. Soc., 94, 292-309.

Lykosov, V.N. and L.N. Gutman, 1972: Turbulent boundary layer above a sloping underlying surface. Izv. Atmos. Oceanic Phys., 8, 462-467.

McLachlan, N.W., 1955: Bessel Functions for Engineers. Second ed. Clarandon Press, Oxford, 188.

Melgarejo, J.W. and J.W. Deardorff, 1974: Stability functions for the boundary layer resistance laws based upon observed boundary layer heights. J. Atmos. Sci., 31, 1324-1333.

Melgarejo, J.W. and J.W. Deardorff, 1975: Revision to 'Stability functions for the boundary layer resistance laws based upon observed boundary-layer heights'. J. Atmos. Sci., 32, 837-839.

Monin, A.S. and S.S. Zilitinkevich, 1974: Similarity theory and resistance laws for the planetary boundary layer. Bound.-Layer Meteor., 7, 391-397.

Sundararajan, A., 1976: Significance of the neutral height scale for the convective, barotropic planetary boundary layer. J. Atmos., Sci., 32, 2285-2287.

Tennekes, H., 1973: A model for the dynamics of the inversion above a convective boundary layer. J. Atmos. Sci., 30, 558-567.

Wyngaard, J.C., O.R. Coté and K.S. Rao, 1974: Modeling the atmospheric boundary layer. Advances in Geophysics, Vol. 18A, Academic Press, 193-211.

Wyngaard, J.C., 1975: Modeling the planetary boundary layer-extension to the stable case. Bound.-Layer Meteor., 9, 441-460.

Yamada, T., 1976: On the Similarity functions A, B and C of the Planetary Boundary Layer. J. Atmos. Sci., 33, 781-793.

Yamada, T., 1978: Prediction of the nocturnal surface inversion height. J. Appl. Meteor., 18, 526-531.

Zilitinkevich, S.S. and D.V. Chalikov, 1968: Determining the universal wind-velocity and temperature profiles in the atmospheric boundary layer. Izv. Atmos. Oceanic Phys., 4, 165-170.

Zilitinkevich, S.S., 1970: The Dynamics of the Atmospheric Planetary Boundary Layer. Gidrometeoizdat Press, Leningrad, 285.

Zilitinkevich, S.S. and J.W. Deardorff, 1974: Similarity theory for the planetary boundary layer of time-dependent height. J. Atmos. Sci., 31, 1449-1452.

Zilitinkevich, S.S. and A.S. Monin, 1974: Similarity theory for the atmospheric boundary layer. Izv. Acad. Nauk SSSR, Fiz. Atmos. Okeana, 10, 587-599.

Zilitinkevich, S.S., 1975: Resistance laws and prediction equations for the depth of the planetary boundary layer. J. Atmos. Sci., 32, 741-752.

APPENDIX

Derivation of the governing equations (1) and (2)

To begin, the general form of the boundary layer equations can be written as

$$\begin{aligned}
&\frac{du_1}{dt} - fv_1 = -\frac{\theta}{\theta_o}\frac{\partial \pi}{\partial x_1} + \frac{\partial}{\partial z_1}\left(K\frac{\partial u_1}{\partial z_1}\right)\\
&\frac{dv_1}{dt} + fu_1 = -\frac{\theta}{\theta_o}\frac{\partial \pi}{\partial y_1} + \frac{\partial}{\partial z_1}\left(K\frac{\partial v_1}{\partial z_1}\right)\\
&\frac{d\theta}{dt} = \frac{\partial}{\partial z_1}\left(K'\frac{\partial \theta}{\partial z_1}\right) \quad (K' = \alpha_H K)\\
&\frac{\partial u_1}{\partial x_1} + \frac{\partial v_1}{\partial y_1} + \frac{\partial w_1}{\partial z_1} = 0\\
&\frac{\theta}{\theta_o}\frac{\partial \pi}{\partial z_1} = -g
\end{aligned} \tag{A1}$$

where

$$\begin{aligned}
&\frac{d}{dt} = \frac{\partial}{\partial t} + u_1\frac{\partial}{\partial x_1} + v_1\frac{\partial}{\partial y_1} + w_1\frac{\partial}{\partial z_1}\\
&\pi = c_p\,\theta_o\left(\frac{p}{p_o}\right)^{R/c_p};\quad p_o = 1000\ \text{mb}
\end{aligned} \tag{A2}$$

The $x_1$, $y_1$ and $z_1$ axes form a right-handed system of Cartesian coordinates (with respect to the horizontal plane) of arbitrary orientation, $u_1$, $v_1$ and $w_1$ are respectively the components of wind velocity along the direction of these axes. $\theta$ is the potential temperature and $\theta_o$ = constant is its mean value.

The other notations are standard in meteorological parlance.

In order to derive more convenient equations than (A1), the following equations for a reference or background atmosphere are introduced (assuming that there is no turbulence):

$$\begin{aligned}
&\frac{DU_1}{Dt} - fV_1 = -\frac{\theta}{\theta_o}\frac{\partial \Pi}{\partial x_1}\\
&\frac{DV_1}{Dt} + fU_1 = -\frac{\theta}{\theta_o}\frac{\partial \Pi}{\partial y_1}\\
&\frac{\partial U_1}{\partial x_1} + \frac{\partial V_1}{\partial y_1} + \frac{\partial W_1}{\partial z_1} = 0\\
&\frac{D\theta}{Dt} = 0\\
&\frac{\theta}{\theta_o}\frac{\partial \Pi}{\partial z_1} = -g
\end{aligned} \tag{A3}$$

where

$$\frac{D}{Dt} = \frac{\partial}{\partial t} + U_1 \frac{\partial}{\partial x_1} + V_1 \frac{\partial}{\partial y_1} + W_1 \frac{\partial}{\partial z_1} \qquad (A4)$$

$$\Pi = c_p \theta_o \left(\frac{P}{P_o}\right)^{R/c_p}$$

Introducing the following definitions and the usual boundary layer approximations:

$$\theta = \Theta + \theta' \; ; \; \pi = \Pi + \pi' \; ; \; u_1 = U_1 + u_1', \; v_1 = V_1 + v_1' \; ; \; w_1 = W_1 + w_1'$$

$$\theta' \ll \Theta \quad ; \; \pi' \ll \Pi \quad ; \; |\Theta - \Theta_o| \ll \Theta_o$$

into (A1), subtracting (A3) from the resultant expressions and neglecting small terms, the following equations are obtained:

$$\frac{\partial u_1'}{\partial t} + u_1 \frac{\partial u_1'}{\partial x_1} + v_1 \frac{\partial u_1'}{\partial y_1} + w_1 \frac{\partial u_1'}{\partial z_1} + u_1' \frac{\partial U}{\partial x_1} + v_1' \frac{\partial U_1}{\partial y_1} + w_1' \frac{\partial U_1}{\partial z_1} - f v_1' =$$

$$= - \frac{\partial \pi'}{\partial x_1} + \frac{\partial}{\partial z_1} \left(K \frac{\partial u_1}{\partial z_1}\right)$$

$$\frac{\partial v_1'}{\partial t} + u_1 \frac{\partial v_1'}{\partial x_1} + v_1 \frac{\partial v_1'}{\partial y_1} + w_1 \frac{\partial v_1'}{\partial z_1} + u_1' \frac{\partial V_1}{\partial x_1} + v_1' \frac{\partial V_1}{\partial y_1} + w_1' \frac{\partial V_1}{\partial z_1} + f u_1' =$$

$$= - \frac{\partial \pi'}{\partial y_1} + \frac{\partial}{\partial z_1} \left(K \frac{\partial v_1}{\partial z_1}\right) \qquad (A5)$$

$$\frac{\partial \theta'}{\partial t} + u_1 \frac{\partial \theta'}{\partial x_1} + v_1 \frac{\partial \theta'}{\partial y_1} + w_1' \frac{\partial \theta'}{\partial z_1} + u_1' \frac{\partial \Theta}{\partial x_1} + v_1' \frac{\partial \Theta}{\partial y_1} + w_1' \gamma = \frac{\partial}{\partial z_1} \left(K \frac{\partial \theta}{\partial z_1}\right)$$

$$\frac{\partial u_1'}{\partial x_1} + \frac{\partial v_1'}{\partial y_1} + \frac{\partial w_1'}{\partial z_1} = 0$$

$$\frac{\partial \pi'}{\partial z_1} = \beta \theta'$$

where

$$\beta = g/\Theta_o \text{ and } \gamma = \frac{\partial \Theta}{\partial z_1}$$

Transforming the $x_1$, $y_1$, $z_1$ system into a new right-handed rectangular $[x, y, z(x_1)]$ system which follows the terrain in such a way that the new x and y axes make small angles $\psi_x$, $\psi_y$ with the $x_1$ and $y_1$ axes, respectively gives (with a good approximation for small slope angles) the following relationships:

$$\frac{\partial}{\partial x_1} \approx \frac{\partial}{\partial x} + \psi_x \frac{\partial}{\partial z}; \; \frac{\partial}{\partial y_1} \approx \frac{\partial}{\partial y} + \psi_y \frac{\partial}{\partial z}; \; \frac{\partial}{\partial z_1} \approx \frac{\partial}{\partial z}$$

$$u \approx u_1; \quad u' \approx u_1' \; ; \; v \approx v_1; \; v' \approx v_1' \qquad (A6)$$

$$w \approx w_1 + u\psi_x + v\psi_y; \quad w' \approx w_1' + u' \psi_x + v' \psi_y$$

Note that in (A6), because of the smallness of $\psi_x$ and $\psi_y$, the approximations $\sin \psi_x \approx \psi_x$, $\sin \psi_y \approx \psi_y$; $\cos \psi_x \approx 1$, $\cos \psi_y \approx 1$ are used. u and v are respectively the wind components along the x and y axes. The z-axis is normal to the terrain and w is the wind component along the same direction.

Introducing the following simplifying assumptions:

$$U_1,\ V_1 = \text{constants},\ W_1 = 0,$$

$$\Theta = \Theta_s + \gamma z,$$

and substituting them together with (A6) into (A5), the following equations are obtained:

$$\frac{\partial u'}{\partial t} + u\frac{\partial u'}{\partial x} + v\frac{\partial u'}{\partial y} + w\frac{\partial u'}{\partial z} - fv' = -\frac{\partial \pi'}{\partial x} - \psi_x \beta\theta' + \frac{\partial}{\partial z}(K\frac{\partial u'}{\partial z})$$

$$\frac{\partial v'}{\partial t} + u\frac{\partial v'}{\partial x} + v\frac{\partial v'}{\partial y} + w\frac{\partial v'}{\partial z} + fu' = -\frac{\partial \pi'}{\partial y} - \psi_x \beta\theta' + \frac{\partial}{\partial z}(K\frac{\partial v'}{\partial z})$$

$$\frac{\partial \theta'}{\partial t} + u\frac{\partial \theta'}{\partial x} + v\frac{\partial \theta'}{\partial y} + w\frac{\partial \theta'}{\partial z} + w'\gamma - (u'\psi_x + v'\psi_y)\gamma = \frac{\partial}{\partial z}(K'\frac{\partial \theta}{\partial z})$$

$$\frac{\partial u'}{\partial x} + \frac{\partial v'}{\partial y} + \frac{\partial w'}{\partial z} = 0 \qquad \text{(A7)}$$

The particular form of the second terms on the right sides of the first two equations in (A7) are from the last expression in (A5). The further simplifying assumptions of steady and horizontal homogeneity in (A7) yield

$$\frac{d}{dz}(K\frac{du'}{dz}) + fv' - \psi_x \beta\theta' = 0$$

$$\frac{d}{dz}(K\frac{dv'}{dz}) - fu' - \psi_y \beta\theta' = 0 \qquad \text{(A8)}$$

$$\frac{d}{dz}(K\frac{d\theta}{dz}) + (\psi_x u' + \psi_y v')\gamma' = 0 \quad (\gamma' = \gamma/\alpha_H)$$

Note that the assumption of horizontal homogeneity together with the boundary condition w = 0 at z = 0 gives from the continuity equation w = w' = 0.

If the (x,y,z) system of (A8) is rotated by an angle $\sigma \leq \pi/2$ **(with z as the axis of rotation)** in such a way that the positive x-axis points along the fall-line vector (see Fig. 1a). The following form of the equations given by Gutman and Melgarejo (1981) is obtained:

$$\frac{d}{dz}\left(K\frac{du''}{dz}\right) + fv'' - \beta\theta'\psi = 0$$

$$\frac{d}{dz}\left(K\frac{dv''}{dz}\right) - fu'' = 0 \qquad \text{(A9)}$$

$$\frac{d}{dz}\left(K\frac{d\theta'}{dz}\right) + \gamma'\psi u'' = 0$$

where

$$u'' = u'\cos\sigma + v'\sin\sigma$$

$$v'' = v'\cos\sigma - u'\sin\sigma$$

and

$$\psi = (\psi_x^2 + \psi_y^2)^{1/2} \; ; \; \sin\sigma = \frac{\psi_y}{\psi} \; ; \quad \cos\sigma = \frac{\psi_x}{\psi}$$

Finally, adding the third equation of (A9) multiplied by $f/(\gamma'\psi)$ to the second gives the equation for q. Next subtracting the third multiplied by $\beta\psi/f$ from the second and adding the result to the first, the following two equations are arrived at:

$$\frac{d}{dz}\left(K\frac{dq}{dz}\right) = 0$$

$$\frac{d}{dz}\left(K\frac{dp}{dz}\right) + i\frac{f}{s}p = 0 \qquad \text{(A10)}$$

where

$$q = v'' + \theta' f/\gamma'\psi$$

$$p = s(v'' - \theta'\beta\psi/f) + iu''$$

and other notations are as in the main text. Note that (1) and (2) in the main text are obtained by substituting sign(f) = -1 (for the Southern Hemisphere) into (A10).

SMHI Rapporter, METEOROLOGI OCH KLIMATOLOGI (RMK)

Nr 1 Thompson, T, Udin, I and Omstedt, A
Sea surface temperatures in waters surrounding Sweden. (1974)

Nr 2 Bodin, S
Development on an unsteady atmospheric boundary layer model. (1974)

Nr 3 Moen, L
A multi-level quasi-geostrophic model for short range weather predictions. (1975)

Nr 4 Holmström, I
Optimization of atmospheric models. (1976)

Nr 5 Collins, W G,
A parameterization model for calculation of vertical fluxes of momentum due to terrain induced gravity waves. (1976)

Nr 6 Nyberg, A
On transport of sulphur over the North Atlantic. (1976)

Nr 7 Lundqvist, J-E and Udin, I
Ice accretion on ships with special emphasis on Baltic conditions. (1977)

Nr 8 Eriksson, B
Den dagliga och årliga variationen av temperatur, fuktighet och vindhastighet vid några orter i Sverige. (1977)

Nr 9 Holmström, I and Stokes, J
Statistical forecasting of sea level changes in the Baltic. (1978)

Nr 10 Omstedt, A and Sahlberg, J
Some results from a joint Swedish-Finnish Sea Ice Experiment, March, 1977. (1978)

Nr 11 Haag, T
Byggnadsindustrins väderberoende, seminarieuppsats i företagsekonomi, B-nivå. (1978)

Nr 12 Eriksson, B
Vegetationsperioden i Sverige beräknad från temperaturobservationer. (1978)

Nr 13 Bodin, S
En numerisk prognosmodell för det atmosfäriska gränsskiktet grundad på den turbulenta energiekvationen.

Nr 14 Eriksson, B
Temperaturfluktuationer under senaste 100 åren. (1979)

Nr 15 Udin, I och Mattisson, I
Havsis- och snöinformation ur datorbearbetade satellitdata - en modellstudie. (1979)

Nr 16 Eriksson, B
Statistisk analys av nederbördsdata. Del I. Arealnederbörd(1979)

Nr 17 Eriksson, B
Statistisk analys av nederbördsdata. Del II. Frekvensanalys av månadsnederbörd. (1980)

Nr 18 Eriksson, B
Årsmedelvärden (1931-60) av nederbörd, avdunstning och avrinning. (1980)

Nr 19 Omstedt, A
A sensitivity analysis of steady, free floating ice. (1980)

Nr 20 Persson, C och Omstedt, G
En modell för beräkning av luftföroreningars spridning och deposition på mesoskala (1980)

Nr 21 Jansson, D
Studier av temperaturinversioner och vertikal vindskjuvning vid Sundsvall-Härnösands flygplats (1980)

Nr 22 Sahlberg, J and Törnevik, H
A study of large scale cooling in the Bay of Bothnia (1980)

Nr 23 Ericson, K and Hårsmar, P-O
Boundary layer measurements at Klockrike. Oct 1977 (1980)

Nr 24 Bringfelt, B
A comparison of forest evapotranspiration determined by some independent methods (1980)

Nr 25 Bodin, S and Fredriksson, U
Uncertainty in wind forecasting for wind power networks (1980)

Nr 26 Eriksson, B
Graddagsstatistik för Sverige (1980)

Nr 27 Eriksson, B
Statistisk analys av nederbördsdata. Del III 200-åriga nederbördsserier. (1981)

Nr 28 Eriksson, B
Den "potentiella" evapotranspirationen i Sverige (1981)

Nr 29 Pershagen, H
Maximisnödjup i Sverige (perioden 1905-70) (1981)

Nr 30 Lönnqvist, O
Nederbördsstatistik med praktiska tillämpningar (Precipitation statistics with practical applications) (1981)

Nr 31 Melgarejo, J W
Similarity theory and resistance laws for the atmospheric boundary layer (1981)

SMHI

SWEDISH METEOROLOGICAL AND HYDROLOGICAL INSTITUTE
Box 923, S-601 19 Norrköping, Sweden. Phone +46 11 10 80 00. Telex 644 00 smhi s

ISSN 0347-2116